MOUNTAIN-PLAINS CONSORTIUM

MPC 18-371 | A. Ghadban and N. Wehbe

Quantifying the Range of Variability in the Flexural Strength of Fiber Reinforced Concrete using Monte Carlo Simulation

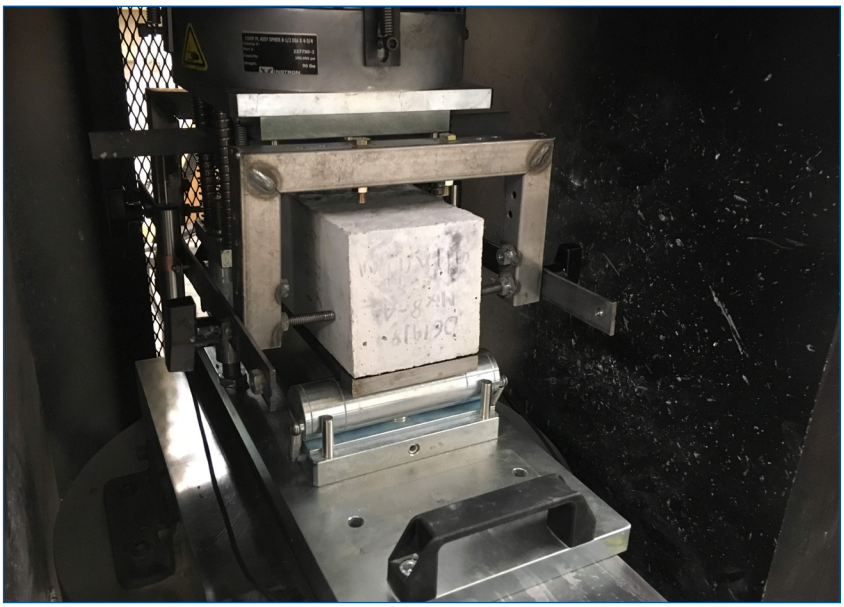

MOUNTAIN-PLAINS CONSORTIUM REGION 8

A University Transportation Center sponsored by the U.S. Department of Transportation serving the Mountain-Plains Region. Consortium members:

Colorado State University
North Dakota State University
South Dakota State University
University of Colorado Denver
University of Denver
University of Utah
Utah State University
University of Wyoming

TECHNICAL REPORT DOCUMENTATION PAGE

1. Report No.	2. Government Accession No.	3. Recipient's Catalog No.
4. Title and Subtitle Quantifying the Range of Variability in the Flexural Strength of Fiber Reinforced Concrete Using Monte Carlo Simulation		**5. Report Date** December 2018 **6. Performing Organization Code**
7. Author(s) Ahmad Ghadban https://orcid.org/0000-0001-8399-0684 Nadim Wehbe https://orcid.org/0000-0002-6266-8378		**8. Performing Organization Report No.** MPC 18-371
9. Performing Organization Name and Address Mountain-Plains Consortium North Dakota State University NDSU Dept. 2880, PO Box 6050 Fargo, ND 58108-6050		**10. Work Unit No.** **11. Contract or Grant No.** Grant #69A3551747108
12. Sponsoring Agency Name and Address U.S. Department of Transportation Research and Special Programs Administration 400 7th Street. SW Washington, DC 20590-0001		**13. Type of Report and Period Covered** Final Report: March 2018-December 2018 **14. Sponsoring Agency Code** USDOT RSPA
15. Supplementary Notes Conducted in cooperation with the U.S. Department of Transportation, Federal Highway Administration.		

16. Abstract

Many laboratory studies have shown erratic results in flexural strength among replicate specimens of Fiber reinforced concrete (FRC). As a result, repeatability of results was very challenging. Given this issue, it would be very difficult for design engineers to make reliable claims about the performance of a certain FRC element in the field. The objective of this project is to provide a better tool for FRC designers to be able to make more robust claims about the performance of an FRC element in transportation infrastructures. This will be carried out through statistically quantifying the range of variability in the flexural strength of FRC using Monte Carlo Simulation. The power of the obtained range of variability prediction tool will be examined through conducting flexural experiments on 8 concrete mixes. These mixes will have randomly selected fiber types, fiber dosages, and other concrete properties in order to examine the power of the developed tool for a wide range of mixes. Ranges of variability associated with several confidence levels will be tested.

17. Key Words	18. Distribution Statement
admixtures, fiber reinforced concrete, flexural strength, mix design, Monte Carlo method	No restrictions. This document is available through the National Technical Information Service, Springfield, VA 22161.

19. Security Classif. (of this report)	20. Security Classif. (of this page)	21. No. of Pages	22. Price
Unclassified	Unclassified	42	Refers to the price of the report. Leave blank unless applicable.

Quantifying the Range of Variability in the Flexural Strength of Fiber Reinforced Concrete using Monte Carlo Simulation

Ahmad A. Ghadban
Post-Doctoral Research Associate
Department of Civil and Environmental Engineering
South Dakota State University
Brooking, SD 57007
Phone: (605) 688-6627
Email: ahmad.ghadban@sdstate.edu

Nadim I. Wehbe
Professor and Department Head
Department of Civil and Environmental Engineering
South Dakota State University
Brooking, SD 57007
Phone: (605) 688-5427
Email: nadim.wehbe@sdstate.edu

December 2018

Acknowledgment

The authors would like to acknowledge the financial support of the Mountain-Plains Consortium (MPC) for funding this study through project MPC-564.

Disclaimer

The contents of this report reflect the views of the authors, who are responsible for the facts and the accuracy of the information presented. This document is disseminated under the sponsorship of the Department of Transportation, University Transportation Centers Program, in the interest of information exchange. The U.S. Government assumes no liability for the contents or use thereof.

ABSTRACT

Many laboratory studies have shown erratic flexural strength results among replicate specimens of fiber reinforced concrete (FRC). As a result, repeatability of results was very challenging. Given this issue, it would be very difficult for design engineers to make reliable claims about the performance of a certain FRC element in the field. The objective of this project is to attempt providing a better tool for FRC designers to be able to make more robust claims about the performance of an FRC element in transportation infrastructures. This was carried out through statistically quantifying the range of variability in the average residual strength (ARS) of FRC using Monte Carlo (MC) simulation. The power of the obtained MC prediction tool was examined through conducting laboratory compressive tests and average residual strength tests on four concrete mixes reinforced with steel fibers. These mixes had randomly selected fiber types, fiber dosages, and other concrete properties in order to examine the power of the developed tool for a wide range of mixes. Results from another four FRC mixes from a previous study were also used. Ranges of variability associated with several confidence levels were tested. Results showed success for some mixes and failure for others.

TABLE OF CONTENTS

LIST OF TABLES

LIST OF FIGURES

EXECUTIVE SUMMARY

Due to its superior tensile properties, fiber reinforced concrete (FRC) has been used in many applications, such as bridge decks, repairs and building beam-column connections. However, since its first use, many laboratory studies have shown erratic flexural strength results among replicate specimens. As a result, repeatability of results was very challenging. Given this issue, it would be very difficult for design engineers to make reliable claims about the performance of a certain FRC element in the field. Consequently, there is a compelling need to mitigate this issue by either eliminating this variability or quantifying it statistically. The research team believes this problem is inherent in FRC and, therefore, is impossible to eliminate. However, we believe the range of variability is possible to quantify statistically. This research involved two main tasks: developing a Monte Carlo (MC) simulation tool to quantify the range of variability in average residual strength values among replicates, and validating the MC prediction tool using experimental data.

The load-deflection relationship was developed using basic mechanics of materials coupled with some simplifying assumptions. Monte Carlo simulation was then used to generate theoretical average residual strength (ARS) values. These values were used to predict a range of variabilities for several confidence levels. Experimental data of eight FRC mixes were used to evaluate the performance of the Monte Carlo prediction tool. Four mixes were prepared by the research team while the data for the other four were obtained from a previous study.

Following are the conclusions of this study.

- Experimental ARS values obtained in this study confirms the issue of significant variability among replicates.
- Monte Carlo simulation for all FRC mixes produced ARS values that conformed with normal distributions.
- Predictions obtained through MC simulation succeeded in quantifying the range of variability in ARS for some mixes but failed for others.
- Oversimplification of the underlying model of the MC simulation is believed to be the main reason behind failed predictions.
- Predictions completely failed for FRC mixes reinforced with synthetic fibers.
- While not a perfect prediction tool, the MC tool developed in this study can still be used to get an idea about the ARS value of FRC members reinforced with steel fibers.

In future attempts, the following modifications to the underlying model could improve the results:

- Use a nonlinear concrete stress profile
- Consider the number of fibers in the tension zone depends on the depth of the neutral axis
- Use a random distribution of fibers instead of uniform distribution
- Consider slippage across the fiber-concrete interface

1. INTRODUCTION

1.1 Project Description

Nationwide, concrete deterioration is one of the major causes of poor performance and shortened life expectancy of concrete roadway infrastructure. Due to the low tensile strength of traditional concrete, reinforced concrete structures often experience cracking and spalling, leading to accelerated corrosion of embedded reinforcement, failure under severe loading, and reduced durability. Fiber-reinforced concrete (FRC) has a solid reputation for superior resistance to crack development and abrasion, along with improvements to strength, ductility, resistance to dynamic loading, and resistance to freeze-thaw effects. Due to these properties, FRC has been used in many applications, such as bridge decks, repairs, and building beam-column connections. However, since its first use, many laboratory studies have shown erratic results in flexural strength among replicate specimens (Chao et al., 2011). As a result, repeatability of results was very challenging.

The high variability in the FRC testing results was mentioned in ACI 544.2R-89 report, "Measurement of Properties of Fiber-Reinforced Concrete" (ACI, 1989). A very recent study sponsored by the South Dakota Department of Transportation (SDDOT) and Mountain Plains Consortium (MPC), "Fiber-Reinforced Concrete for Structure Components," also showed similar results to previous studies in terms of extreme variabilities in flexural strength results among replicate specimens (Ghadban et al., 2018). A previous study conducted by Armelin and Banthia attempted to predict this variability, but only considered compressive strength and pullout force-versus-slip relationships as inputs for the model. Additionally, during each run, they used the same fiber orientation for every fiber, which is not representative of actual FRC members. Their study also lacked sufficient data and did not produce any algorithm that could be used by designers to predict this variability (Armelin & Banthia, 1997). To the best knowledge of the research team, there have been no other studies tackling this issue.

Given this issue, it would be very difficult for design engineers to make reliable claims about the performance of a certain FRC element in the field. Consequently, there is a compelling need to mitigate this issue by either eliminating this variability or quantifying it statistically. The research team believes this problem is inherent in FRC and, therefore, is impossible to eliminate. However, the team believes the range of variability is possible to quantify statistically.

1.2 Objectives

The goal of this project is to provide a better tool for FRC designers to be able to make more robust claims about the performance of any FRC element in transportation infrastructures. The following objectives are designed to achieve this goal.

- Statistically quantify the range of variability in the flexural strength of FRC using Monte Carlo simulation.
- Experimentally validate the obtained range of variability by conducting flexural tests.

2. MATHEMATICAL DERIVATION

2.1 Load-Deflection Relationship

The research team predicts that the variability in the experimental results among replicates is most likely due to the random orientation each fiber exhibits in a given cross-section. Consequently, the load vs. deflection relationship was derived assuming random orientation of fibers within the cross-section. However, the uniform distribution assumption seemed to be reasonable and was, therefore, retained. To simplify the derivation, the actual cross-section was converted to an equivalent cross-section where all fibers within a layer were combined into a single fiber (Figure 2.1).

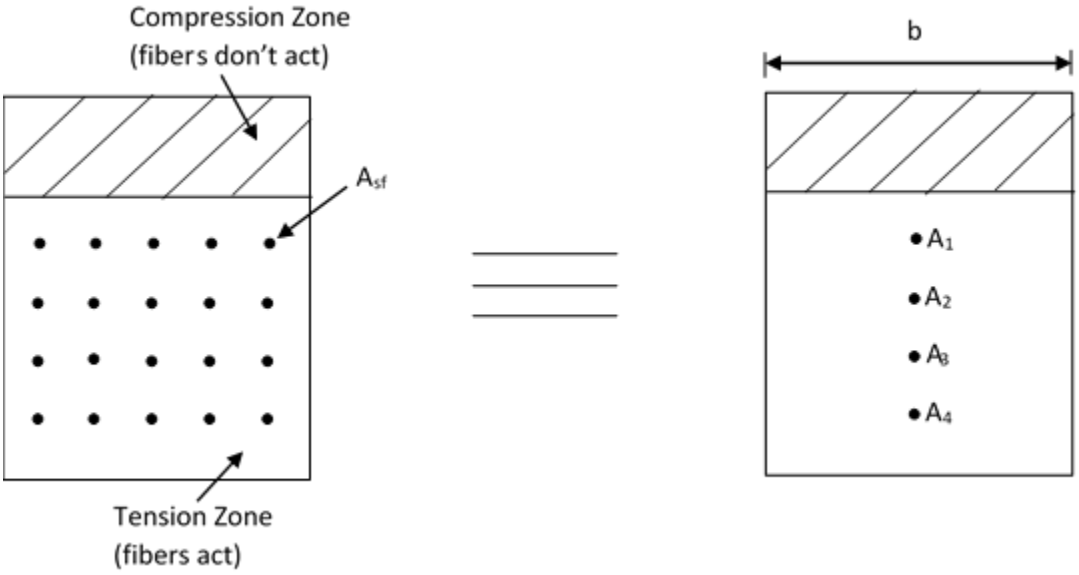

Figure 2.1 Combining fibers within each layer

Where:

A_{sf} = Area of a single fiber
A_i = Total area in each layer of fibers
b = Width of cross-section

Due to the difference in orientation among the fibers, each A_i could, in reality, have an eccentricity about the minor axis. However, since the loading is applied about the major axis and the vertical deflection is the only deflection of concern, this eccentricity is irrelevant and, therefore, was ignored during the derivation.

To account for the orientation of each fiber, A_{sf} was multiplied by a random number, n_i, between 0 and 1. A_i can then be obtained using the following equation.

$$A_i = n_1 A_{sf} + n_2 A_{sf} + \cdots = \sum_{j=1}^{N_1} n_j A_{sf}$$

Where:

N_1 = Number of fibers in each layer = $\frac{\sqrt{V_f}}{\sqrt{A_{sf}}} b$

V_f = Total volume fraction of fibers

Since N_1 could be a non-integer, define K_1 as N_1 rounded to the nearest integer. Therefore, A_i can be written as follows.

$$A_i = \frac{\sum_{j=1}^{K_1} n_j}{K_1} N_1 A_{sf}$$

To further simplify the derivation, the fiber layers were further combined into a single fiber, A_f, as shown in Figure 2.2.

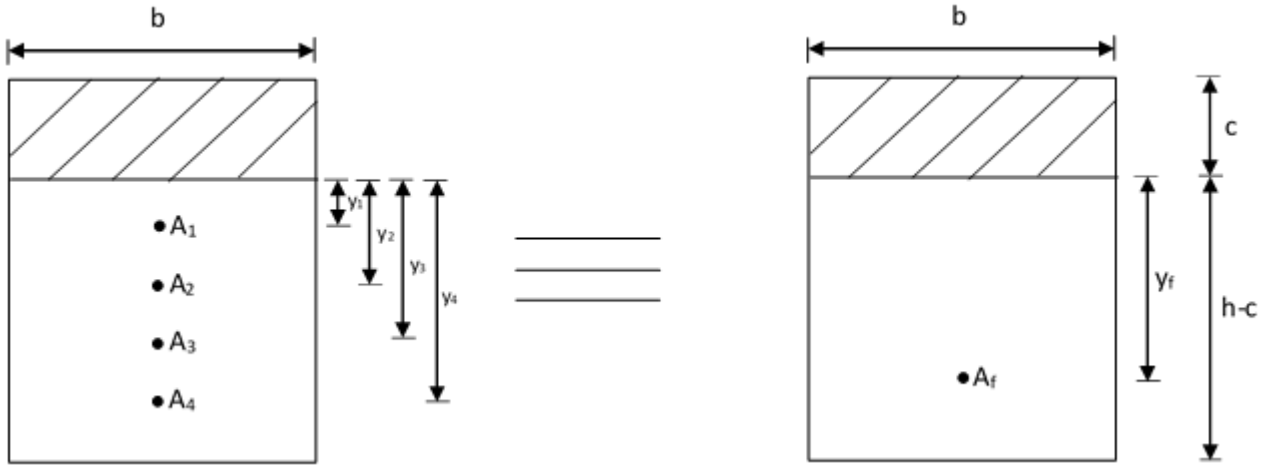

Figure 2.2 Combining layers into a single fiber

Where:

y_i = Distance from each layer of fibers to the neutral axis
y_f = Distance from the resultant fiber to the neutral axis
h = Depth of cross-section
c = Depth of neutral axis

A_f can be calculated as follows.

$$A_f = A_1 + A_2 + \cdots = \sum_{i=1}^{N_2} A_i$$

Where:

N_2 = Number of fiber layers = $\frac{\sqrt{V_f}}{\sqrt{A_{sf}}}(h - c)$

Since N_2 could be a non-integer, define K_2 as N_2 rounded to the nearest integer. Therefore, A_f can be written as follows.

$$A_f = \frac{\sum_{i=1}^{K_2} A_i}{K_2} N_2$$

y_f can then be obtained using moment of area around the neutral axis:

$$A_f y_f = A_1 y_1 + A_2 y_2 + \cdots = \sum_{i=1}^{N_2} A_i y_i = \frac{\sum_{i=1}^{K_2} A_i y_i}{K_2} N_2$$

Substituting A_f into the equation, we get:

$$\frac{\sum_{i=1}^{K_2} A_i}{K_2} N_2 y_f = \frac{\sum_{i=1}^{K_2} A_i y_i}{K_2} N_2 \xrightarrow{yields} y_f = \frac{\sum_{i=1}^{K_2} A_i y_i}{\sum_{i=1}^{K_2} A_i}$$

y_i can be obtained using the distances between the fiber layers. Since uniform distribution is assumed, the distance between every fiber layer and the one adjacent to it is $\frac{h-c}{K_2+1}$. Therefore, y_i can be calculated using the following equation.

$$y_i = i\frac{h-c}{K_2+1}$$

y_f can then be rewritten as:

$$y_f = \frac{\sum_{i=1}^{K_2} A_i i \frac{h-c}{K_2+1}}{\sum_{i=1}^{K_2} A_i} = \frac{h-c}{K_2+1}\frac{\sum_{i=1}^{K_2} iA_i}{\sum_{i=1}^{K_2} A_i}$$

One can notice that to obtain N_2, we need c, which in turn depends on A_f that requires N_2. This requires an iterative procedure. To avoid that, we can further simplify the derivation by choosing an average c, call it c_a, only for the purposes of calculating N_2. c_a can be obtained from the average case where the orientations of the fibers are such that 50% of the total area of the fibers in the tension zone will be acting at the center of the tension zone, as shown in Figure 2.3.

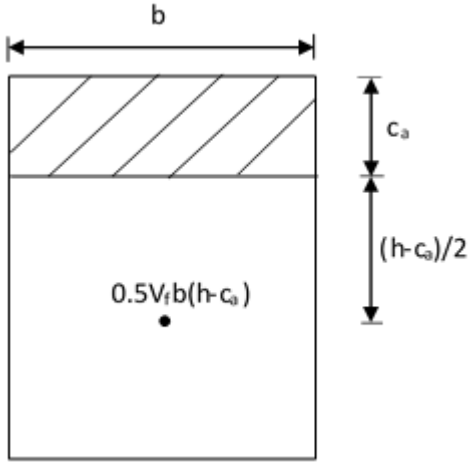

Figure 2.3 An average case to calculate c_a

To find c_a, we first draw the strain and stress profiles (Figure 2.4). Since the specimen is never loaded to failure in an average residual strength (ARS) test, concrete will, for the most part, act in the linear stress zone. Consequently, a linear stress profile is assumed.

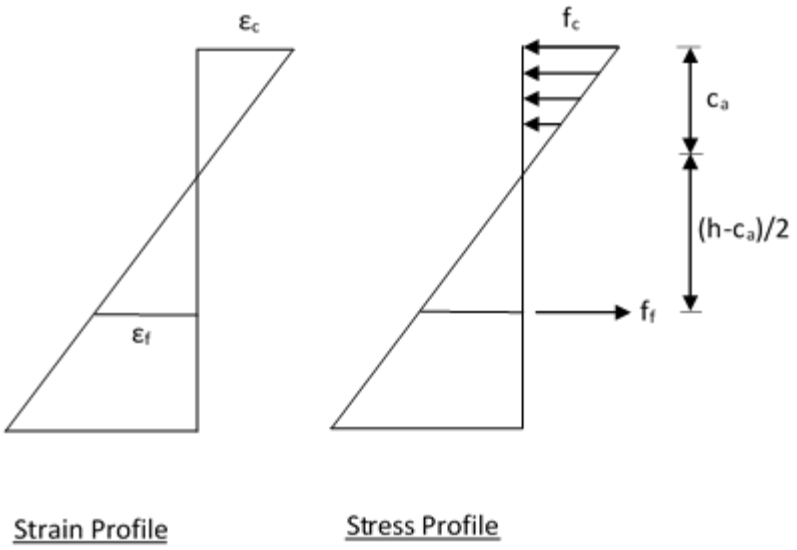

Figure 2.4 Strain and stress profiles

Where:

ε_c = Concrete strain at the top fiber of the cross-section
ε_f = Fiber strain
f_c = Concrete stress at the top fiber of the cross-section
f_f = Fiber stress

Using similar triangles, the following strain relation can be obtained.

$$\frac{\varepsilon_f}{\frac{h-c}{2}} = \frac{\varepsilon_c}{c} \xrightarrow{yields} \varepsilon_f c = \frac{h-c}{2}\varepsilon_c$$

From the stress profile, the following relation can be obtained.

$$\sum F = 0 \xrightarrow{yields} 0.5 c_a b E_c \varepsilon_c = 0.5 V_f b (h - c_a) E_f \varepsilon_f$$

Where:

E_c = Modulus of elasticity of concrete
E_f = Modulus of elasticity of fibers

Substituting this equation back into the previous one results in the following quadratic equation in c_a.

$$\left[\frac{E_c}{0.5 V_f E_f} - 1\right] {c_a}^2 + 2hc_a - h^2 = 0$$

This equation can be solved to obtain c_a as follows.

$$c_a = \frac{-1 + \sqrt{\frac{E_c}{0.5 V_f E_f}}}{\frac{1}{h}\left[\frac{E_c}{0.5 V_f E_f} - 1\right]}$$

For further simplicity, the cross-section can be converted to an equivalent cross-section with an equivalent fiber area, A_{eq}, located at the middle of the tension zone, as shown in Figure 2.5.

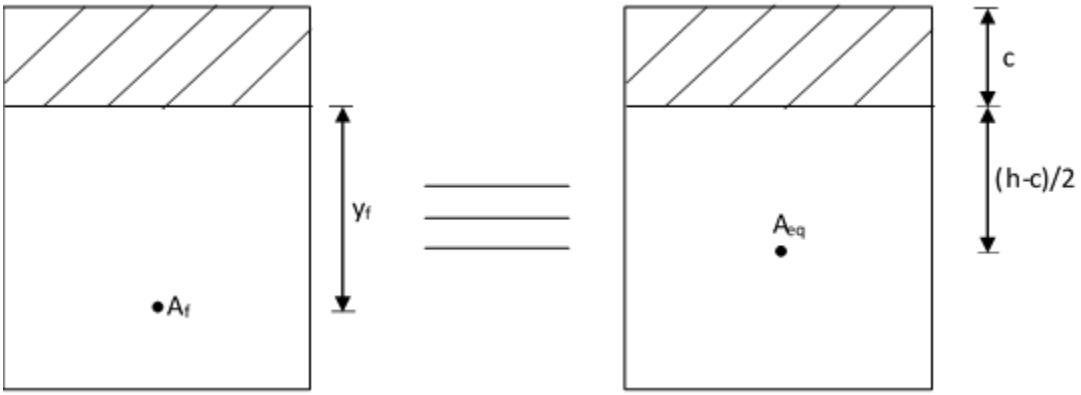

Figure 2.5 An equivalent cross-section

A_{eq} can be obtained using moment of area around the neutral axis as follows.

$$A_{eq}\frac{h-c}{2} = A_f y_f \xrightarrow{yields} A_{eq} = \frac{2}{h-c}A_f\frac{h-c}{K_2+1}\frac{\sum_{i=1}^{K_2} iA_i}{\sum_{i=1}^{K_2} A_i} \xrightarrow{yields} A_{eq} = \frac{2A_f}{K_2+1}\frac{\sum_{i=1}^{K_2} iA_i}{\sum_{i=1}^{K_2} A_i}$$

For the ARS test setup shown in Figure 2.6, the midspan deflection, δ, is:

$$\delta = \frac{23PL^3}{1296E_c I_{cr}}$$

Where:

P = Applied load
L = Clear span of beam
I_{cr} = Cracked moment of inertia

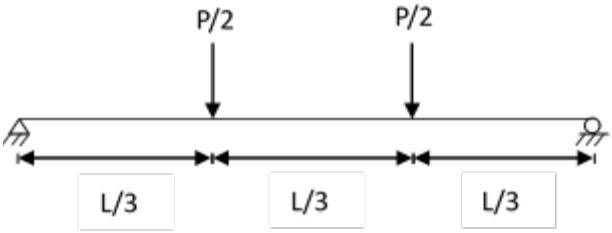

Figure 2.6 Average residual strength testing setup sketch

The cracked moment of inertia is used because the ARS testing setup requires the beam to be pre-cracked prior to measuring ARS. Assuming A_{eq} has not yielded, the cracked moment of inertia can be calculated in a similar manner to conventional reinforced concrete, yielding the following equation.

$$I_{cr} = \frac{bc^3}{3} + \frac{E_f}{4E_c}A_{eq}(h-c)^2$$

c can be obtained in a similar manner to c_a, resulting in the following expression.

$$c = \frac{-1 + \sqrt{1 + \frac{4bE_c h}{A_{eq}E_f}}}{\frac{2bE_c}{A_{eq}E_f}}$$

Equating internal moment to external moment yields the following equation, which can be used to calculate ε_f to check yielding of A_{eq}.

$$A_{eq}E_f\varepsilon_f\left(\frac{h}{2} + \frac{c}{6}\right) = \frac{PL}{6}$$

If A_{eq} has yielded, the previous equation becomes:

$$A_{eq}f_{fy}\left(\frac{h}{2} + \frac{c}{6}\right) = \frac{PL}{6} \xrightarrow{yields} c = \frac{PL}{A_{eq}f_{fy}} - 3h$$

Where:

f_{fy} = Yield strength of fibers

Due to yielding, E_f approaches zero, resulting in the following cracked moment of inertia expression.

$$I_{cr} = \frac{bc^3}{3} \xrightarrow{yields} I_{cr} = \frac{b\left[\frac{PL}{A_{eq}f_{fy}} - 3h\right]^3}{3}$$

The P-δ relation can then be rewritten as follows.

$$\delta = \frac{23PL^3}{1296E_c\frac{b\left[\frac{PL}{A_{eq}f_{fy}} - 3h\right]^3}{3}} \xrightarrow{yields} (AP - B)^3 - CP = 0$$

Where:

A = $\frac{L}{A_{eq}f_{fy}}$

B = 3h

C = $\frac{23L^3}{432E_c b\delta}$

This cubic equation can be solved to obtain:

$$P = \frac{\sqrt[3]{\frac{2}{3}}C}{D} + \frac{D}{\sqrt[3]{18}A^3} + \frac{B}{A}$$

Where:

D = $\sqrt[3]{9A^5BC + \sqrt{3}\sqrt{27A^{10}B^2C^2 - 4A^9C^3}}$

The following procedures can be used to construct the P-δ relation for a given beam specimen.

1. Fibers are assigned random orientations.
2. Equivalent fiber area is calculated.
3. Assuming the equivalent fiber has not yielded, c is calculated.

4. Cracked moment of inertia is calculated.
5. For a given midspan deflection, the applied load is calculated.
6. Equivalent fiber strain is calculated.
7. If equivalent fiber has not yielded, stop and use P-δ relation obtained in step 5. Otherwise, calculate the applied load for a given midspan deflection using the equation that assumes a yielding equivalent fiber.

All fiber properties necessary to compute theoretical ARS for the tested specimens were obtained from the manufacturer, and are shown in Table 3.1. The only concrete property needed is the modulus of elasticity, which was obtained from experimental results shown in Table 4.2

2.1 Monte Carlo Simulation

For each FRC mix, the derived P-δ relation was used to compute theoretical ARS for 1 million virtual specimens. For each specimen, fiber orientations were randomly selected. The data were then plotted to confirm adherence to normal distributions. Means and standard deviations were then calculated to obtain upper and lower limits for several confidence intervals. Table 2.1 shows the confidence levels that were looked at in this study. The experimental data were then checked for adherence to the upper and lower limits of each confidence interval.

Table 2.1 Limits of confidence intervals used in this study

Confidence Level (%)	Limits (x ±Standard Deviation)
38.29	0.5
68.27	1
86.64	1.5
95.45	2
98.76	2.5
99.73	3
99.95	3.5
99.99	4

3. EXPERIMENTAL METHODOLOGY

This section discusses the experimental laboratory testing plan for this study. The testing plan implemented standard ASTM testing procedures. The purpose of the experimental work was to obtain the average residual strength for multiple FRC mix designs in order to verify the predictions made by the Monte Carlo simulation.

3.1 Selection of Fibers

Two steel fibers with different yield strengths, supplied by Bekaert, were tested. Table 3.1 shows the two fibers that were selected, along with certain properties for each.

Table 3.1 List of selected fibers for experimental evaluation

Fiber	Dramix 4D	Dramix 3D
Length (in)	2.36	2.36
Equivalent Diameter (in)	0.035	0.035
Aspect Ratio*	65	65
Specific Gravity	8.32	8.04
Tensile Strength (ksi)	232.1	168.2
Modulus of Elasticity (ksi)	29007.5	29007.5
Recommended Dosage Rate (lb/yd^3)	25 minimum	25 minimum

* Aspect Ratio = fiber length divided by equivalent fiber diameter

3.2 Materials and Mix Design

Four FRC mixes were tested in this study. All mixes utilized Type I Portland cement. One mix contained quartzite coarse aggregate, while the other three contained limestone. Quartzite had a specific gravity of 2.64 and an absorption of 0.33%, while limestone had a specific gravity of 2.74 and an absorption of 1.29%. The natural sand had a specific gravity of 2.65 and an absorption of 1.1%. A high range water reducer (HRWR) was used in two of the four mixes. It was an ADVA CAST 575 supplied by Grace Construction Products. Table 3.2 shows the mixing proportions for each of the four mixes.

Table 3.1 FRC mix design for all mixes

Material	Mix1	Mix2	Mix3	Mix4
Type I Cement (lb/yd^3)	800	800	929	929
Coarse Aggregate Type	Limestone	Quartzite	Limestone	Limestone
Coarse Aggregate (lb/yd^3)	1355	1330	929	929
Fine Aggregate (lb/yd^3)	1355	1330	1857	1857
Water (lb/yd^3)	400	400	325	325
w/c	0.5	0.5	0.35	0.35
HRWR (oz/cwt)	None	None	11	11
Fiber Type	Dramix 4D	Dramix 3D	Dramix 3D	Dramix 4D
Fiber Dosage lb/yd^3 (% by volume)	100 (0.71)	50 (0.37)	120 (0.89)	65 (0.46)
Total Volume of Mix (ft^3)	2.25	2.6	2.25	2.25

The percentage by volume of fibers is defined as the ratio of the volume of fibers to the total volume of the composite concrete mix (Abdalla, et al., 2008). Therefore, the equation (Equation 3.1) to determine the volume fraction of fibers can be written as follows:

$$V_f = \frac{V_{fib}}{V_{total}} = \frac{V_{fib}}{V_{mat} + V_{fib}} = \frac{(m_{fib}/\rho_{fib})}{(m_{mat}/\rho_{mat}) + (m_{fib}/\rho_{fib})} = \frac{(m_{fib})(\rho_{mat} * \rho_{fib})}{\rho_{fib}(m_{mat} * \rho_{fib} + m_{fib} * \rho_{mat})}$$

$$\therefore V_f = \frac{(m_{fib})(\rho_{mat})}{(m_{mat})(\rho_{fib}) + (m_{fib})(\rho_{mat})} \quad \textbf{Eq. 3.1}$$

Where:

$V_f = volume\ fraction\ of\ fibers$
$V_{fib} = volume\ of\ fibers$
$m_{fib} = mass\ of\ fibers\ [lb]$
$\rho_{fib} = density\ of\ fibers\ \left[{}^{lb}/_{yd^3}\right]$
$V_{mat} = volume\ of\ concrete\ materials\ (excluding\ fibers)$
$m_{mat} = mass\ of\ concrete\ materials\ [lb]$
$\rho_{mat} = density\ of\ concrete\ materials\ \left[{}^{lb}/_{yd^3}\right]$

The volume fraction of fibers is a measurement widely used for specifying the fiber dosage rate.

3.3 Laboratory Tests

The tests selected for this study are shown in Table 3.3.

Table 3.3 Selected material tests

Type of Test	Test Name	Standard/Source
Fresh Concrete	Density (Unit Weight)	ASTM C138
	Slump of Hydraulic-Cement Concrete	ASTM C143
	Air Content of Freshly Mixed Concrete by the Pressure Method	ASTM C231
	Temperature of Freshly Mixed Hydraulic-Cement Concrete	ASTM C1064
Hardened Concrete	Compressive Strength of Cylindrical Concrete Specimens	ASTM C39
	Average Residual-Strength of Fiber-Reinforced Concrete	ASTM C1399

The testing procedures for each fresh concrete and hardened concrete specimen are discussed in Section 3.3.2 and Section 3.3.3, respectively.

3.3.1 Sample Preparation

Each specimen was prepared according to ASTM C192 and ACI Committee 544 (1989). ASTM C192 provided basic concrete sample preparation guidelines, while ACI Committee 544 provided various alterations that should be followed when working with FRC. The following sections discuss the standard methods used for mixing, placing, consolidating, and curing each specimen, along with any alterations in procedures specified by ACI Committee 544.

3.3.1.1 Mixing

Concrete mixing was performed in the concrete laboratory in Crothers Engineering Hall on the campus of SDSU. A ½-cubic-yard electric concrete drum mixer was used, and is shown in Figure 3.1.

Figure 3.1 ½-cubic-yard capacity concrete drum mixer

The literature review showed there are limited differences between mixing Portland Cement Concrete (PCC) and FRC (Ghadban et al., 2018). Currently, there is no specific method for mixing FRC. Therefore, the method specified by ASTM C192 for mixing PCC was used for mixing the FRC batches; the fibers were added to the mix at the end of the procedure, as recommended by fiber manufacturers. Once all of the other concrete materials were mixed together, as specified by ASTM C192, the fibers were added to the mixer and allowed additional mixing time. The adopted mixing procedures are as follows:

1) Prior to starting rotation of the mixer, add the coarse and fine aggregates and approximately one-third of the mixing water.
2) Start the mixer then add the cement and the remaining water with the mixer running.
3) After all of the ingredients are in the mixer, mix for three minutes.
4) Stop the mixer and allow the concrete to rest for three minutes.
5) Prior to starting the mixer, add the fibers by evenly distributing them above the surface of the resting concrete (shown in Figure 3.2).
6) Start the mixer, then add the water reducer with the mixer running, and mix for five minutes.

Figure 3.2 Distribution of fibers on the surface of the resting concrete, prior to the final five minutes of mixing

The specified mixing time following the addition of fibers was determined based on a previous FRC study (Ghadban et al., 2018).

3.3.1.2 Placement

For the experimental tests listed in Table 1.4, ASTM C192 specifies the amount of lifts that should be used for filling specimen forms of different shape and dimensions. Table 3.4 displays the number of lifts that was used for each of the tests.

Table 3.4 Number of lifts required for each experimental test

	Specimen Shape and Dimensions	Number of Lifts Required
Slump	Standard slump cone	3
Air Content	Standard air content measure	3
Compressive Strength	6″ x 12″ cylinder	2
Average Residual Strength	4″ x 4″ x 14″ beam	1

3.3.1.3 Consolidation

According to ACI Committee 544, internal or external vibration must be used for consolidating FRC specimens to avoid preferential fiber alignment and non-uniform distribution of fibers. However, rodding was used for the fresh concrete tests, as per ASTM Standards (Figure 3.3).

Figure 3.3 Rodding during a concrete slump test

ASTM C143 and ASTM C231 were used for determining the amount of consolidation required for each of the respective material tests. Internal vibration was selected, since it was a common method based on a previous FRC study (Ghadban et al., 2018). Table 3.5 shows the required number of rod or vibrator insertions performed for each lift, as specified by ASTM C143 and ASTM C231.

Table 3.5 Number of vibrator insertions required per lift for each experimental test

	Specimen Shape and Dimensions	Number of Insertions Required Per Lift
Slump	Standard slump cone	Rodding: 25
Air Content	Standard air content measure	Rodding: 25
Compressive Strength	6″ x 12″ cylinder	Vibration: 2
Average Residual Strength	4″ x 4″ x 14″ beam	Vibration: 3

According to ASTM C192, the rod/vibrator head should penetrate into the lower layer of concrete by approximately 1 inch. Sufficient vibration was usually considered to have been achieved as soon as the surface of the concrete became relatively smooth, and large air bubbles ceased to break through the top surface, as can be seen in Figure 3.4. For consistency, the vibrator was inserted for three to five seconds for each insertion. After each lift was rodded or vibrated, the outsides of the mold were tapped at least 10 times by a rubber mallet (Figure 3.5). ASTM C192 also states that for any beam molds, the vibrator should be inserted at intervals not exceeding 6 inches along the center line of the specimen's long dimension. This requirement was also followed during the consolidation. After consolidation, the surface of the specimen was smoothed out using a wooden trowel, as shown in Figure 3.6
.

Figure 3.4 Hand-held spud vibrator in use

Figure 3.5 Use of rubber mallet to obtain final consolidation efforts of the concrete

Figure 3.6 Finishing using a wooden trowel

3.3.1.4 Curing

As revealed in a previous FRC study (Ghadban et al., 2018), curing techniques for FRC do not differ from that of PCC. Therefore, the curing method specified by ASTM C192 was used for all of the hardened concrete material test specimens. All specimens were water-cured by submerging them in a water tank, as shown in Figure 3.7, at 73.5 ± 3.5°F until the time of testing.

Figure 3.7 Water tank used to cure all hardened specimens

3.3.2 Fresh Concrete Testing

The fresh concrete tests, including slump, air content, unit weight, and concrete temperature, were performed according to the respective ASTM standard, and are discussed in the following sections.

3.3.2.1 Slump

The slump of each concrete mix was measured according to ASTM C143. There were no alterations made to this procedure. A typical slump test performed by the research team is shown in Figure 3.8.

.

Figure 3.8 Measurement of the concrete slump, according to ASTM C143

3.3.2.2 Air Content

The air content of each concrete mix was evaluated according to ASTM C231. No alterations to the specified test method were made. The air meter used is shown in Figure 3.9.

Figure 3.9 Air meter used to determine the concrete's air content, according to ASTM C231

3.3.2.3 Fresh Unit Weight

The fresh unit weight of each concrete mix was evaluated according to ASTM C138 (2013). No alterations to the specified test method were made. The weight measurement of a known volume of concrete was used to determine the unit weight.

3.3.2.4 Concrete Temperature

The concrete temperature of each concrete mix was evaluated according to ASTM C1064 (2012). No alterations to the specified test method were made.

3.3.3 Hardened Concrete Testing

3.3.3.1 Compressive Strength

Five standard 6″ x 12″ cylinders were used for each concrete mix to determine the compressive strength according to ASTM C39 (2012). The ends of the cylinders were capped with high-strength sulfur capping compound according to ASTM C617 (2012). Capping the cylinders provided a level surface for uniform loading of the specimen.

The tests were performed under load-control settings at a rate of 35 ± 7 psi/sec, as specified by ASTM C39. The modulus of elasticity of the cylinders was also determined during compression testing. Shown in Figure 3.10 is an 8″ extensometer from Instron used to accurately measure the axial strain; it is clamped onto a concrete cylinder at four points. Two clamping points were 2″ above the bottom of the cylinder, while the other two points were 2″ below the top of the cylinder. The entire compressive strength testing setup is shown in Figure 3.11
.

Figure 3.10 8″ Extensometer used to measure the compressive strain of a concrete cylinder during testing, according to ASTM C39

Figure 3.11 Compressive strength testing setup

Theoretical modulus of elasticity was calculated in accordance with Equation 2.

$$E_c = 33{w_c}^{1.5}\sqrt{f'_c} \quad \textbf{Eq. 3.2}$$

Where:

$E_c = Modulus\ of\ elasticity\ [psi]$
$w_c = Concrete\ unit\ weight\ [lb/ft^3]$
$f'_c = Compressive\ strength\ [psi]$

3.3.3.2 Average Residual Strength

Five beams with dimensions of 4″ x 4″ x 14″ were used for each concrete mix to measure the average residual strength according to ASTM C1399. The specimens were simply supported with a clear span of 12″. Third-point loading was used under a displacement-control setting. The deflection of the beam was measured using two deflectometers from Instron. These deflectometers were accurate to $1x10^{-6}$ inches and had a range of 0.6 inches. A yoke was secured to the specimen directly above the supports and was used to hold the deflectometers in place. This setup helped ensure accurate measurement of the net mid-span deflection regardless of any concrete crushing or specimen seating or twisting on its supports. There was one deflectometer mounted on each side of the specimen at mid-span. The values recorded from each

gauge were averaged to determine the net mid-span deflection. Figure 3.12 and Figure 3.13 show the test setup, along with the yoke and LVDT locations, respectively.

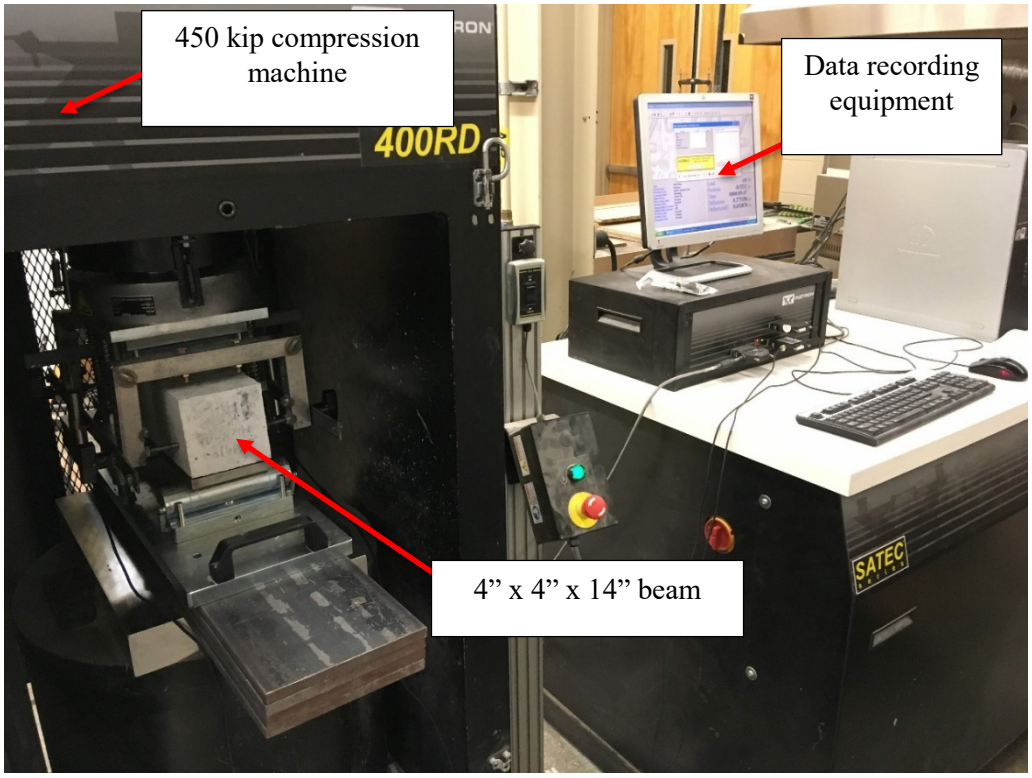

Figure 3.12 Average residual strength testing setup

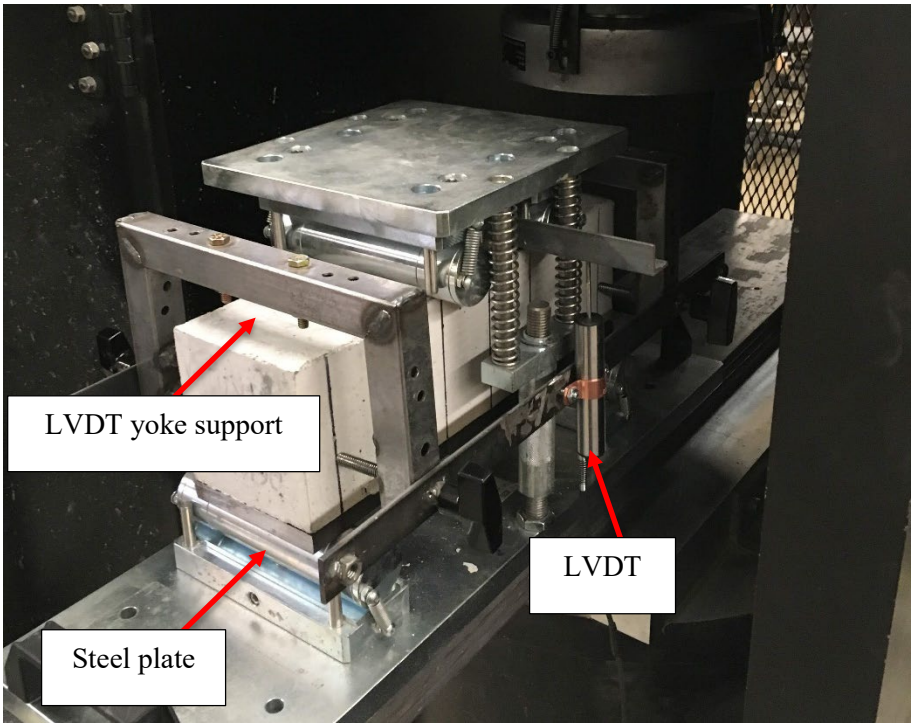

Figure 3.13 Closeup on an average residual strength testing setup

Initially, the specimen was placed on top of a 4″ x ½″ x 14″ steel plate (Figure 3.13) and centered onto the flexural support apparatus. An initial loading rate of 0.025 ± 0.005 in/min was used until reaching a deflection of 0.008 inches, which corresponds to the first crack in the beam (Figure 3.14). After that, the specimen was unloaded and the steel plate was removed from beneath the concrete. Once the steel plate was removed, the concrete specimen was placed back on the support apparatus. Using the same loading rate as before, the specimen was loaded to a deflection of 0.05 inches. During the second stage of loading, the load at 0.02, 0.03, 0.04, and 0.05 inches deflection was recorded, as specified by ASTM C1399 and shown in Figure 3.15. The average residual strength for each beam was calculated using Equation 3, and then a mean average residual strength for each set of beams was calculated.

$$ARS = \frac{(P_A + P_B + P_C + P_D)L}{4bd^2} \quad \textbf{Eq. 3.3}$$

Where:

$ARS = Average\ residual\ strength\ [psi]$
$P_A + P_B + P_C + P_D = Sum\ of\ recorded\ loads\ at\ specified\ deflections\ [lb]$
$L = Span\ length\ [in]$
$b = Specimen\ width\ [in]$
$d = Specimen\ depth\ [in]$

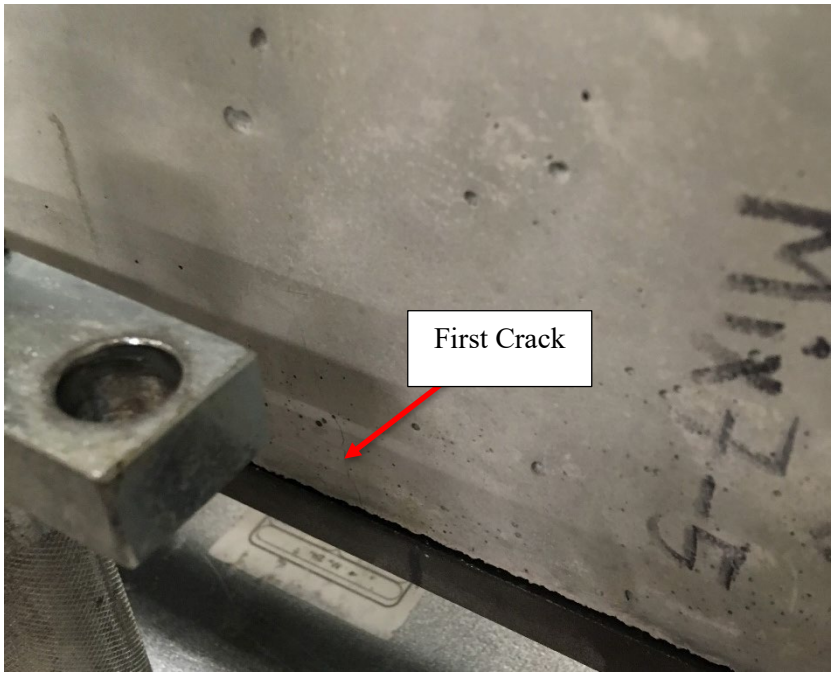

Figure 3.14 First crack in an average residual strength specimen

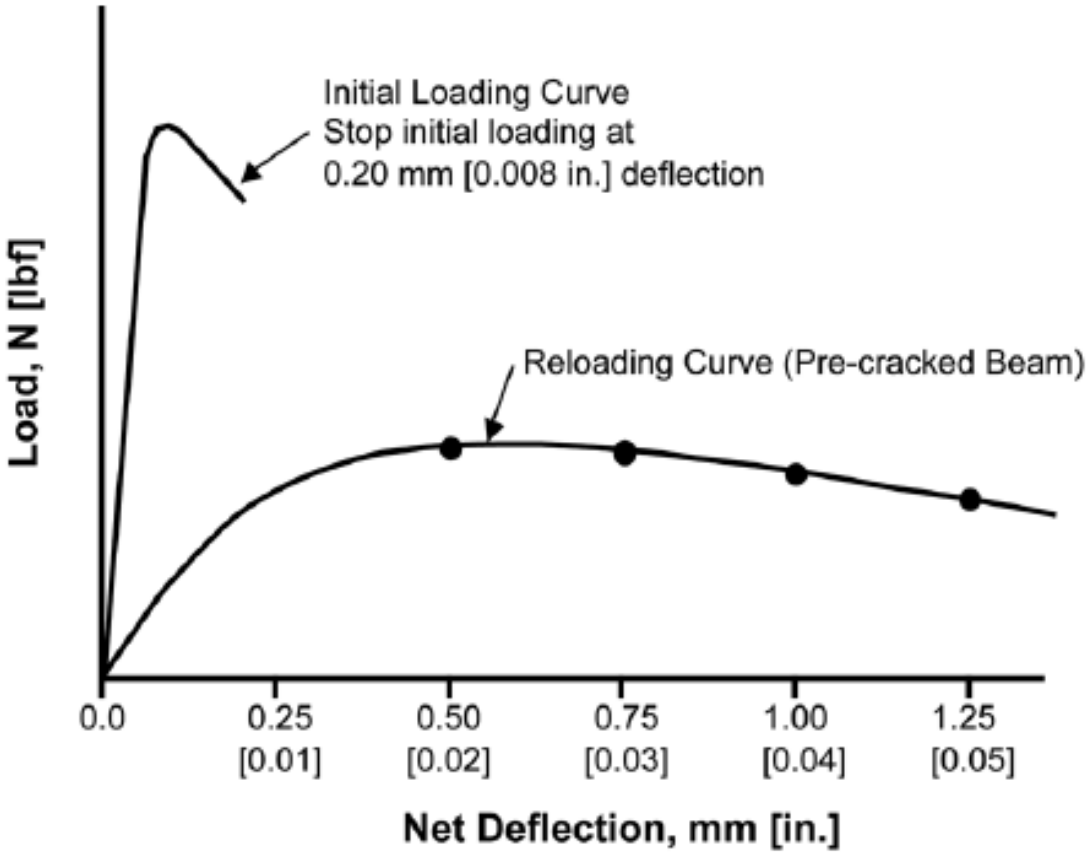

Figure 3.15 Typical load-deflection curves for the average residual strength test (ASTM C1399, 2010)

4. RESULTS AND DISCUSSION

This section presents the results obtained from fresh and hardened concrete experiments conducted on the four FRC mixes. It also compares experimental ARS values to theoretical ones obtained from a Monte Carlo simulation. Furthermore, the results of four additional FRC mixes obtained from a previous study (Ghadban et al., 2018) were also used to validate theoretical predictions.

4.1 Fresh and Hardened Properties

rs (i.e., flexural properties).

Table 4.1 and Table 4.2 summarize fresh and hardened properties of all four FRC mixes conducted in this study. One can observe from Table 1.8 the extremely erratic nature of the ARS values among replicates within an FRC mix. This variability among replicates is not as pronounced in the case of compressive strength and modulus of elasticity values. This is a major indication of the amount of uncertainty associated with properties that depend on the action of fibers (i.e., flexural properties).

Table 4.1 Summary of fresh concrete properties

Mixture ID	Fresh Air Content (%)	Unit Weight (lb/ft^3)	Slump (in)	Temperature (^{o}F)
Mix1	2.6	152.1	6.25	78.5
Mix2	2.6	149.1	8.5	76
Mix3	2.7	154.6	9.5	65
Mix4	2.3	146.2	8.875	66

Table 4.2 Summary of hardened concrete properties

Mixture ID	Specimen Number	Compressive Strength (psi)	Modulus of Elasticity (ksi)	Average Residual Strength (psi)
Mix1	1	7296.0	4868.8	1299.8
	2	6992.2	4766.3	1163.0
	3	7795.4	5032.6	752.3
	4	N/A	N/A	570.0
	5	N/A	N/A	1029.4
	Average	7361.2	4889.2	962.9
Mix2	1	6921.1	4742.0	714.8
	2	6623.3	4638.9	656.7
	3	7076.4	4794.9	272.8
	4	6675.3	4657.0	475.8
	5	N/A	N/A	451.4
	Average	6824.0	4708.2	514.3
Mix3	1	11344.9	6071.2	1440.5
	2	10736.6	5906.2	1161.1
	3	10616.7	5873.1	1240.3
	4	11286.6	6055.6	1311.6
	5	11802.2	6192.4	1561.4
	Average	11157.4	6019.7	1343.0
Mix4	1	10450.1	5826.9	1073.9
	2	10619.2	5873.8	1036.4
	3	10249.9	5770.8	1141.4
	4	9435.1	5536.7	1202.3
	5	10873.1	5943.6	1472.8
	Average	10325.5	5790.4	1185.4

4.2 Monte Carlo Simulation

The theoretical ARS values computed for the four mixes prepared in this study, along with the other four mixes obtained from a previous study (Ghadban et al., 2018), were clearly conforming with normal distributions.

Figure 4.1 shows an example of a probability density function for one of the mixes.

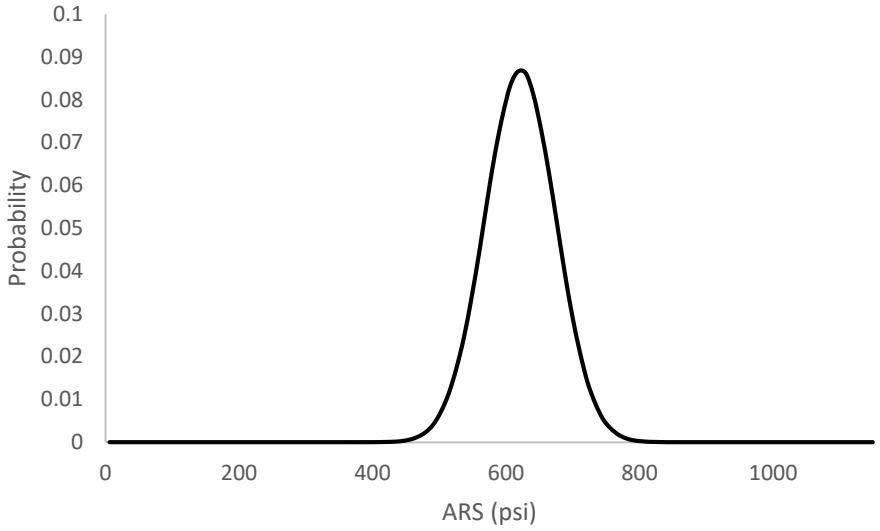

Figure 4.1 Probability density function for Mix2

Since all data are adhering to normal distributions, one can obtain lower and upper limits for each confidence level using Table 2.1. Table 4.3 presents an example of confidence intervals for several confidence levels for one of the mixes. At a first glance, even for a confidence level of 99.99%, it seems that the confidence interval is not significantly big considering the variability observed among the replicates in Table 4.2.

Table 4.3 Lower and upper limits for various confidence levels for Mix1

Confidence Level (CL), %	Lower Limit (LM), psi	Upper Limit (UL), psi
38.29	1090.2	1160.1
68.27	1055.3	1195.0
86.64	1020.4	1229.9
95.45	985.4	1264.8
98.76	950.5	1299.8
99.73	915.6	1334.7
99.95	880.7	1369.6
99.99	845.7	1404.5
100	0	2059.6

The following section compares the experimental results with the confidence intervals obtained from the MC simulation.

4.3 Experimental vs. Theoretical

Figure 4.2 through Figure 4.5 show the experimental ARS values along with the confidence intervals obtained through MC simulation for each of the FRC mixes examined in this study. In each figure's legend, CL stands for "confidence level." While Figure 4.4 shows good confinement of the experimental ARS values of Mix3 within the 99.73% confidence interval, other mixes produced ARS values that were even outside the 99.99% confidence interval. Figure 4.5 shows underestimation by an MC simulation of the actual ARS values, while Figure 4.2 and Figure 4.3 show overestimation for some specimens. This shows that an MC simulation can sometimes be very conservative, while in other occasions be detrimental.

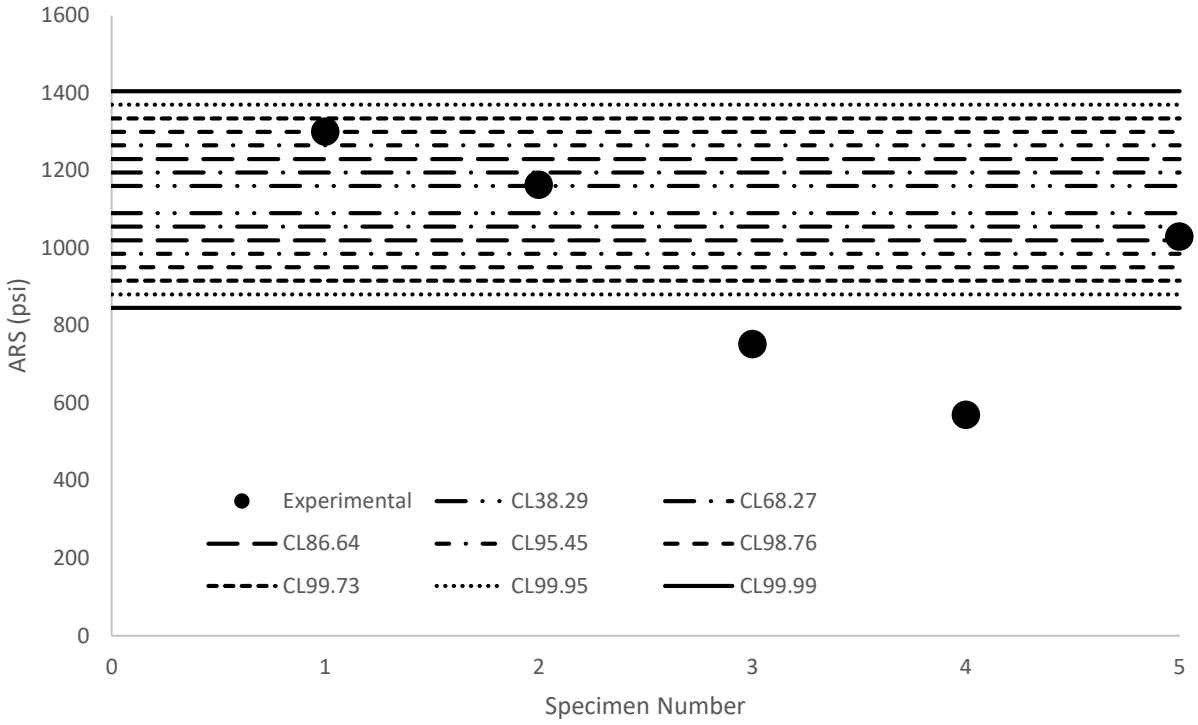

Figure 4.2 Experimental ARS vs. MC Simulation confidence intervals for Mix1

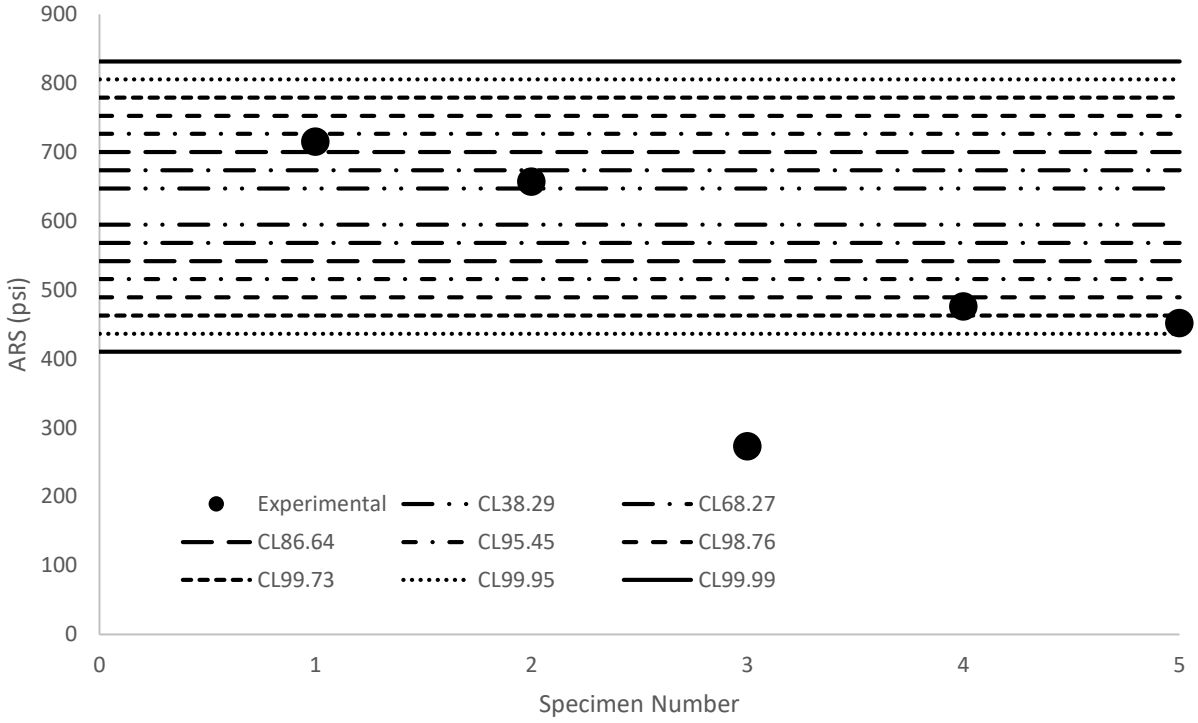

Figure 4.3 Experimental ARS vs. MC simulation confidence intervals for Mix2

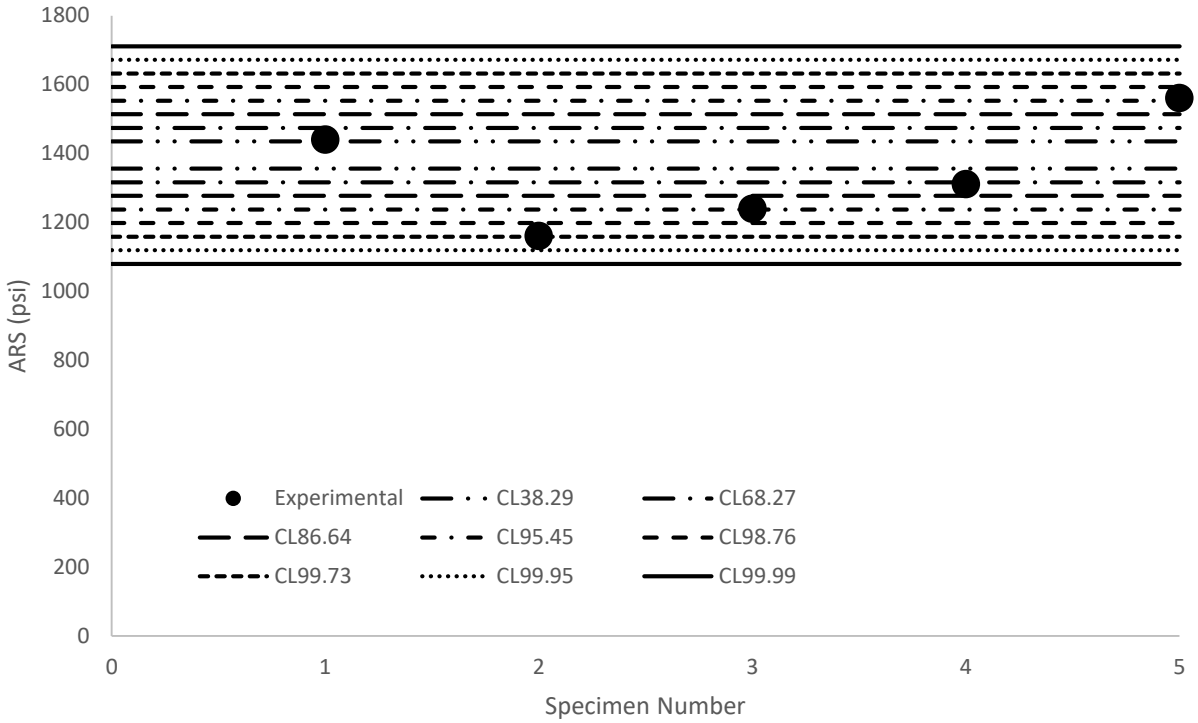

Figure 4.4 Experimental ARS vs. MC simulation confidence intervals for Mix3

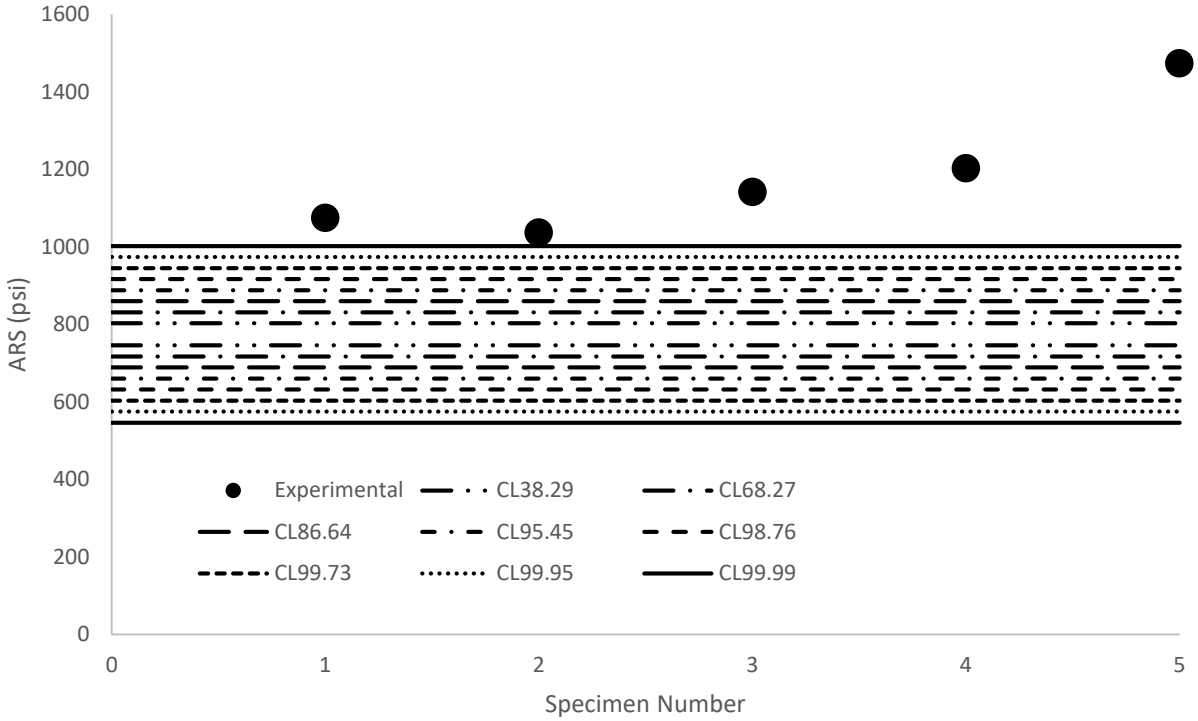

Figure 4.5 Experimental ARS vs. MC simulation confidence intervals for Mix4

Similar results were found for the other mixes obtained from a previous study (Ghadban et al., 2018) as shown in Figure 4.6 through Figure 4.9. These mixes are called here Mix5, Mix6, Mix7, and Mix8. For more information about these mixes, refer to the previous study (Ghadban et al., 2018). In the previous study, these mixes are labeled DR-1, DR-2, DR-3, and DR-4, respectively. Figure 4.6 and Figure 4.7 show relatively good prediction of the experimental ARS values, while Figure 4.8 and Figure 4.9 show a drastic overestimation by MC simulation.

This discrepancy between the MC predictions and the actual ARS values could be attributed to the oversimplification of the underlying model used in the MC simulation. It might be possible to obtain better predictions by assuming a nonlinear concrete stress profile. Eliminating the assumption of "fixed number of fibers in the tension zone regardless of the location of the neutral axis" could also improve ARS predictions. In addition to the random orientation, incorporating random distribution into the model could also help capture outliers by increasing the range of the confidence interval. The research team believes a possible suspect behind the occasional overestimation of ARS values is the assumption of "perfect bond between fibers and concrete." Incorporating slippage across the concrete-fiber interface into the model could help improve its prediction power. While these modifications to the underlying model could indeed improve predictions, they can drastically complicate the theoretical derivation process. It should be noted that all of the aforementioned FRC mixes contain steel fibers. The research team tried to apply MC simulation on FRC mixes reinforced with synthetic fibers; however, the predictions were extremely poor, significantly underestimating ARS values. It is possible another reinforcing mechanism is associated with synthetic fibers.

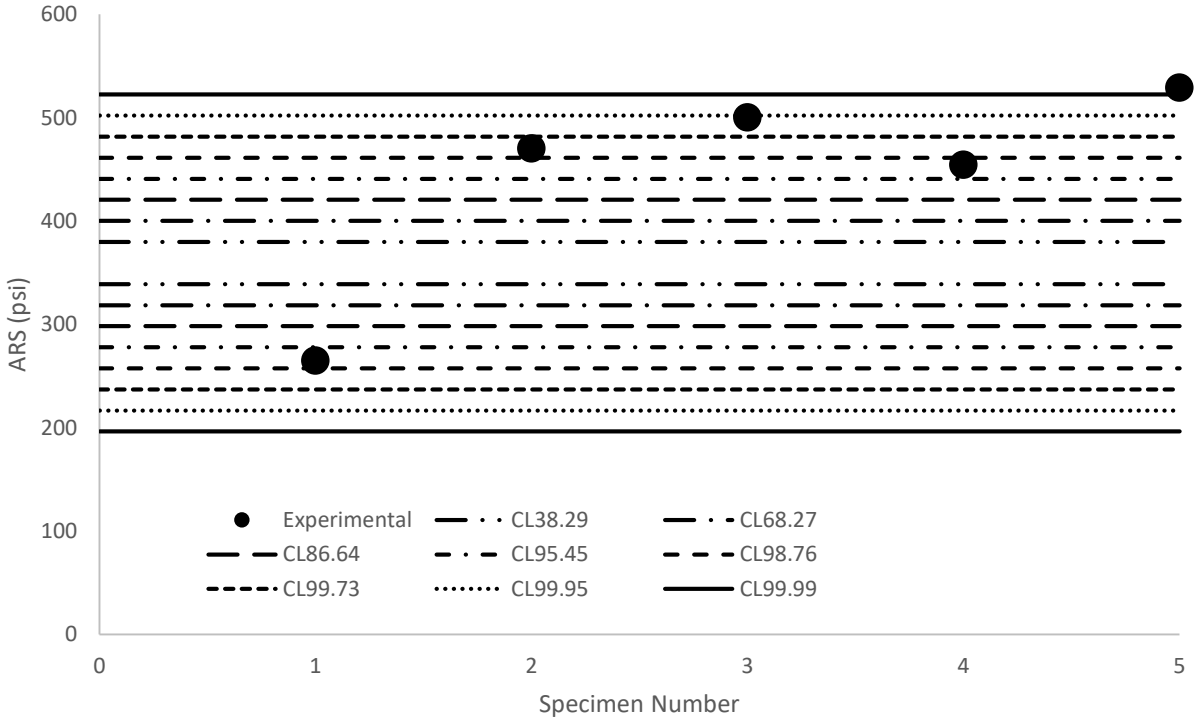

Figure 4.6 Experimental ARS vs. MC simulation confidence intervals for Mix5

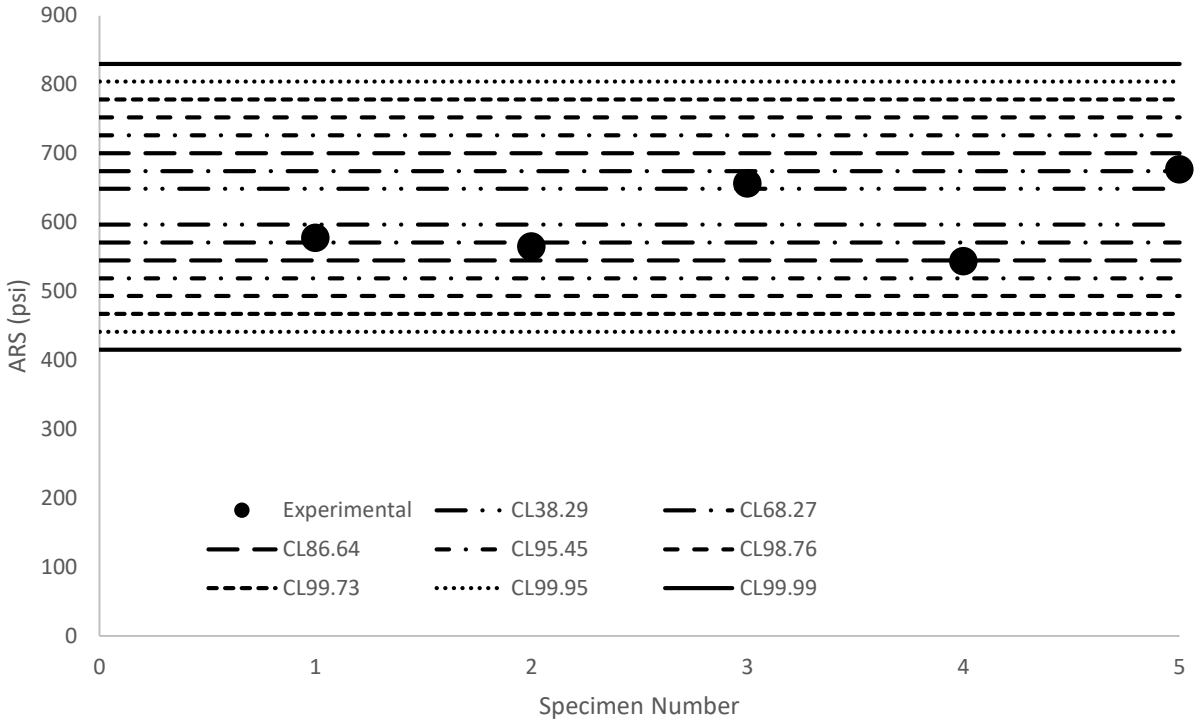

Figure 4.7 Experimental ARS vs. MC simulation confidence intervals for Mix6

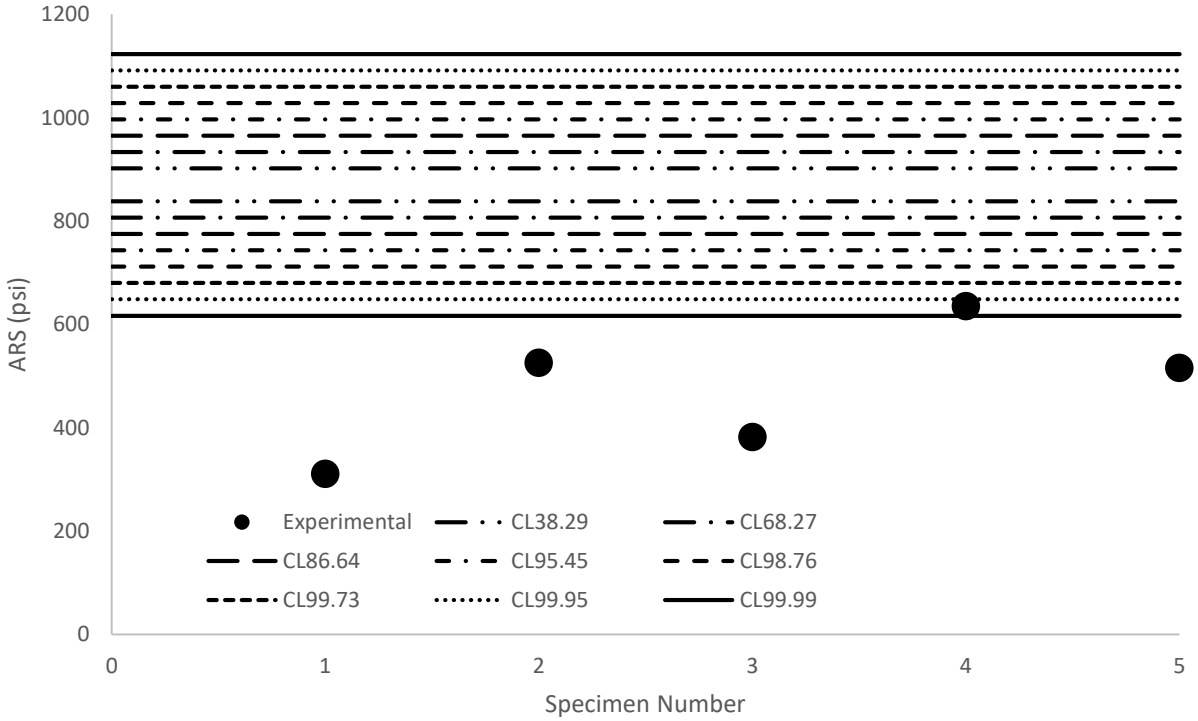

Figure 4.8 Experimental ARS vs. MC simulation confidence intervals for Mix7

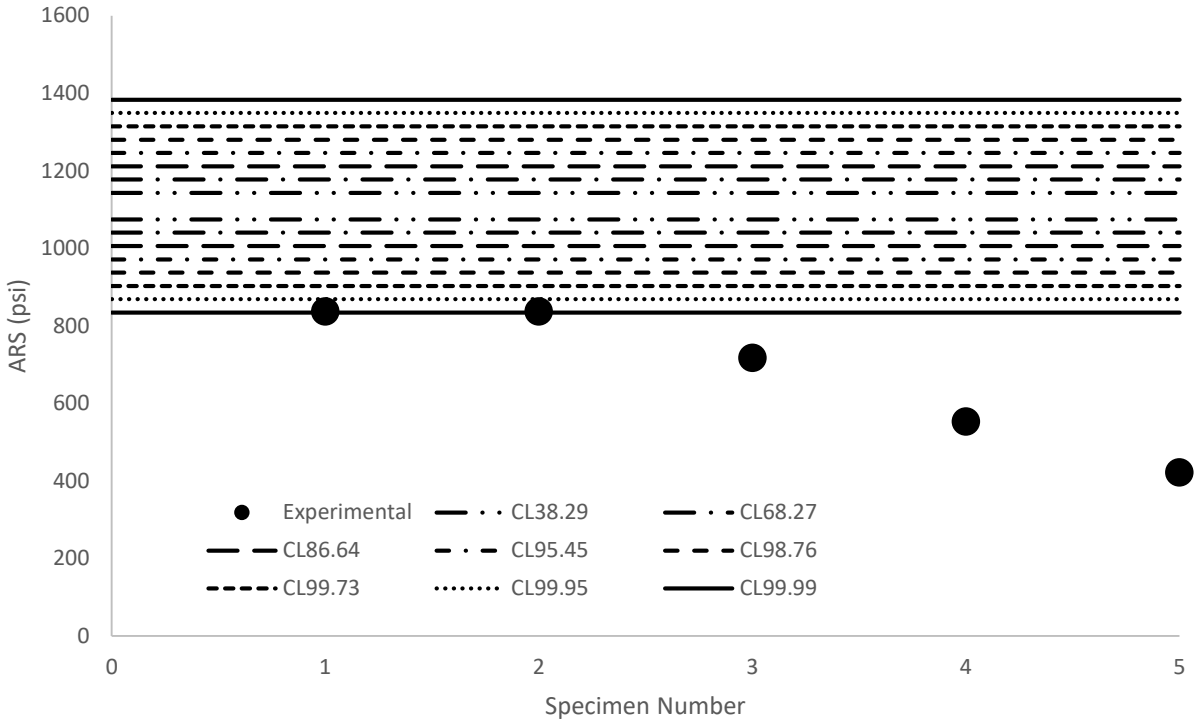

Figure 4.9 Experimental ARS vs. MC simulation confidence intervals for Mix8

5. CONCLUSIONS AND RECOMMENDATIONS

The study presented in this report was conducted to attempt predicting the range of variability in the ARS of FRC using Monte Carlo simulation, and validate these predictions using experimental data. The following conclusions and recommendations are based on the results of this study.

5.1 Conclusions

- Experimental ARS values obtained in this study confirm the issue of significant variability among replicates.
- Monte Carlo simulation for all FRC mixes produced ARS values that conformed with normal distributions.
- Predictions obtained through MC simulation succeeded in quantifying the range of variability in ARS for some mixes but failed for others.
- Oversimplification of the underlying model of the MC simulation is believed to be the main reason behind failed predictions.
- Predictions completely failed for FRC mixes reinforced with synthetic fibers.
- While not a perfect prediction tool, the MC tool developed in this study can still be used to get an idea about the ARS value of FRC members reinforced with steel fibers.

5.2 Recommendations

For future attempts, the following modifications to the underlying model could improve the results:

- Nonlinear concrete stress profile
- Number of fibers in the tension zone depends on the depth of the neutral axis
- Random distribution of fibers instead of uniform distribution
- Slippage across the fiber-concrete interface

6. REFERENCES

Abdalla, F. H., Megat, M. H., Sapuan, M. S., and Sahari, B. B. (2008). "Determination of Volume Fraction Values of Filament Wound Glass and Carbon Fiber-Reinforced Composites." *ARPN Journal of Engineering and Applied Sciences*, Vol. 3, No. 4, Pg. 7-11.

American Concrete Institute (ACI) Committee 544. (1989). Measurement of Properties of Fiber-Reinforced Concrete. Rep. No. ACI 544.2R-89. Farmington Hills, MI: American Concrete Institute.

Armelin, H. S., Banthia, N. (1997). "Predicting the Flexural Postcracking Performance of Steel Fiber Reinforced Concrete from the Pullout of Single Fibers." *ACI Materials Journal*, 94 (1), 18-31.

ASTM. (2010). ASTM C1399/C1399M-10 Standard Test Method for Obtaining Average Residual-Strength of Fiber-Reinforced Concrete. West Conshohocken, PA: ASTM International.

ASTM. (2010). ASTM C231/C231M-10 Standard Test Method for Air Content of Freshly Mixed Concrete by the Pressure Method. West Conshohocken, PA: ASTM International.

ASTM. (2012). ASTM C1064/C1064M-12 Standard Test Method for Temperature of Freshly Mixed Hydraulic-Cement Concrete. West Conshohocken, PA: ASTM International.

ASTM. (2012). ASTM C143/C143M-12 Standard Test Method for Slump of Hydraulic-Cement Concrete. West Conshohocken, PA: ASTM International.

ASTM. (2012). ASTM C39/C39M-12a Standard Test Method for Compressive Strength of Cylindrical Concrete Specimens. West Conshohocken, PA: ASTM International.

ASTM. (2013). ASTM C138/C138M-13 Standard Test Method for Density (Unit Weight), Yield, and Air Content (Gravimetric) of Concrete. West Conshohocken, PA: ASTM International.

Chao, S., Cho, J., Karki, N. B., Sahoo, D. R., & Yazdani, N. (2011). FRC Performance Comparison: Uniaxial Direct Tensile Test, Third-Point Bending, and Round Panel Test. Tech. No. SP-276-5. Texas Department of Transportation.

Ghadban, A. A., Wehbe, N. I., & Underberg, M. (2018). "Effect of Fiber Type and Dosage on Flexural Performance of FRC for Highway Bridges." *ACI Materials Journal*, Vol. 115, No. 3, Pg. 413-424.